Material selection of the SPD Beam-Beam Counter scintillation detector prototype

A. M. Zakharov[a,*], *F. A. Dubinin*[c,a], *A. Yu. Isupov*[b], *V. P. Ladygin*[b], *A. D. Manakonov*[a], *G. A. Nigmatkulov*[a,†], *S. G. Reznikov*[b], *P. E. Teterin*[a], *A. V. Tishevsky*[b], *I. S. Volkov*[b], *A. O. Zhurkina*[a]

[a] National Research Nuclear University MEPhI (Moscow Engineering Physics Institute), Kashirskoe Shosse 31, 115409 Moscow, Russia

[b] Veksler and Baldin Laboratory of High Energy Physics, Joint Institute for Nuclear Research, Dubna, Moscow region, 141980 Russia

[c] Lebedev Physical Institute of the Russian Academy of Sciences (RAS), Leninsky Avenue 53, 119991, Moscow, Russia

The Spin Physics Detector is an experiment at NICA designed to study the spin structure of the proton and deuteron and the other spin-related phenomena using polarized beams. Two endcap detector wheels of scintillator-based Beam-Beam Counters (BBCs) will be installed symmetrically aside from the interaction point and will serve as a tool for beam diagnostics including local polarimetry. The selection of material combinations for BBC is presented using scintillation tiles with different material combinations of the BBC prototype. The influence of the light collection was studied using matted and covered with Tyvek tiles. Different fibers (Saint-Gobain Crystals BCF91AS, BCF92S, and Kuraray Y-11), as well as different optical cements (CKTN type E, OK-72) were used. The prototypes were tested with cosmic rays and radioactive source using SensL SiPM readout.

PACS: 44.25.+f; 44.90.+c

Introduction

The Spin Physics Detector is an experiment at NICA (JINR, Dubna) designed to study the spin structure of the proton and deuteron and the other spin-related phenomena using a unique possibility to operate with polarized proton and deuteron beams at a collision energy up to 27 GeV and a luminosity up to 10^{32} cm^{-2} s^{-1} (Fig. 1). Physics with unpolarized beams is also possible, especially at the first stage of NICA operation with reduced luminosity and collision energy of the proton and ion beams.

Two endcap detector wheels of scintillator-based Beam-Beam Counters (BBCs) are planned to be located in front of the TOF system of the SPD setup. The main goals of the Beam-Beam Counters are the local polarimetry at SPD, based on the measurements of the azimuthal asymmetries in the

*E-mail: arsimi@yandex.ru

†Currently at: Univeristy of Illinois Chicago, West Harrison St. 1200, 60607, Chicago, Illinois, USA

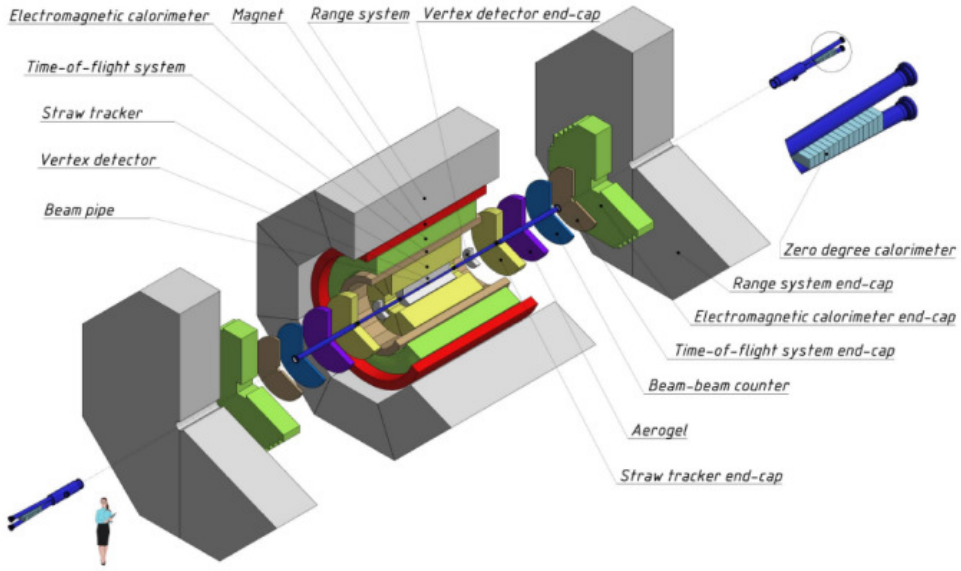

Fig. 1: General layout of the SPD setup

inclusive production of charged particles in the collisions of transversely polarized proton beams, and the monitoring of the beam collisions similarly to STAR EPD [1]. Geometry of SPD BBC has been updated in a collaboration of MEPhI and JINR SPD groups in order to increase radial granularity and is different from the one presented in SPD conceptual design [2]. Schematic view of the updated SPD Beam-Beam Counter sector, produced from the tiles of fast plastic scintillator, is presented in Fig. 2.

FERS-5200 front-end readout system

The SPD BBC is designed to have 16 sectors with 25 tiles in each sector (Fig. 2a) in one wheel. Each tile is a separate signal source that should be read using silicon photomultiplier (SiPM), connected to WLS fiber. The amount of readout channels leads us to use CAEN FERS-5200 front-end readout system, that was designed for large detector arrays [3]. Each board holds 64 channels and includes Front-End electronics, ADC, trigger logic, synchronization, local memory, and readout interface. Concentrator DT5215 is used for the possibility of expanding the number of channels to 8192. Although CAEN FERS-5200 has an internal coincidence circuit (CC), an external trigger has been used for measurements with cosmic rays. Internal CC is used for radioactive source measurements. The tile system with external trigger – two 10×10 cm^2 scintillators, located under and over tile system, with Hamamatsu H10720-110 PMTs readout and time resolution ~650 ps.

Materials selection

Technical design stage is dedicated to the material selection for the detector. The detector prototype is made of polystyrene scintillator tiles with

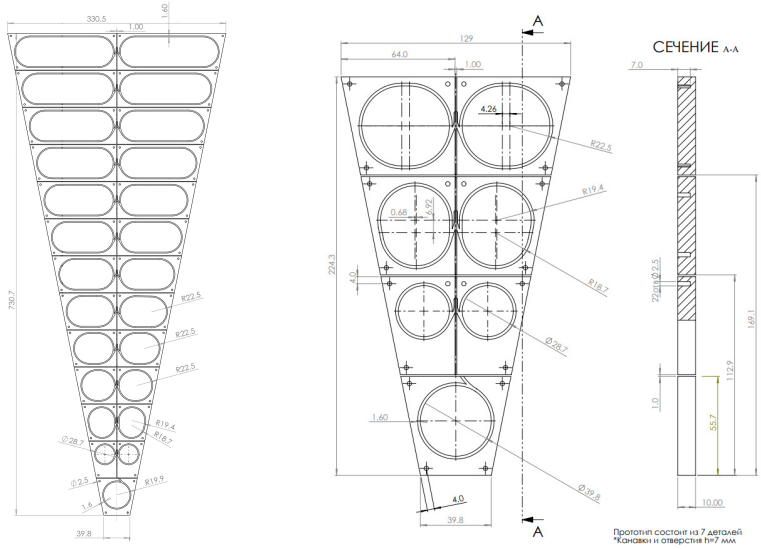

(a) (b)

Fig. 2: Geometry of one BBC sector

the machined grooves for WLS fibers bedding. The light collection strongly depends on a surface coating of the scintillator. Photons reflect from the coating layer and are trapped inside the volume until collected by the fiber or absorbed by the absorption centers (defects, traps). Additionally, the light collection depends on optical cement that fixes a fiber inside the tile. Also, optical cement is used to get rid of the air gap, that spoils the light collection, too. The refractive indexes of the scintillator, the optical cement and the fiber should match to each other to ensure minimal reflection during the light passing through the tile. Finally, spectral characteristics of the WLS should match to the scintillator's ones for better light collection.

Before the measurements, the SiPM calibration was performed. CAEN SP5601 led driver was used as stable signal source, 4 SensL $3 \times 3\,mm^2$ SiPMs were read by 4 DT5202 channels. The DT5202 channels were found to have different signal amplification, so signal amplitudes variation from channel to channel for different SiPMs caused not only by difference of bias voltage, but also by difference between FERS-5200 channels. Thus, the signal amplitude depends on the SiPM and on the channel in use, so each SiPM was assigned to its own channel.

In the measurement, we used the scintillator tiles (by Uniplast Vladimir [4], [5]) covered with a white acrylic paint (so-called "matted") and the tiles double covered with a unique non-woven material baced on high-density polyethylene continuous filaments (Tyvek). The BBC prototype uses 4 first lines of tiles (from bottom to top), the scheme is presented in Fig. 2b. Here the bottom one is designated as the central one, and others are named in accordance with their position relative to the center tile: first, second and third line, correspondingly.The tiles of 1 and 3 lines, covered by Tyvek and matted, with the WLS BCF92 and the grooves filled with the optical cement CKTN MED type E were used to perform the comparison. The Convolution

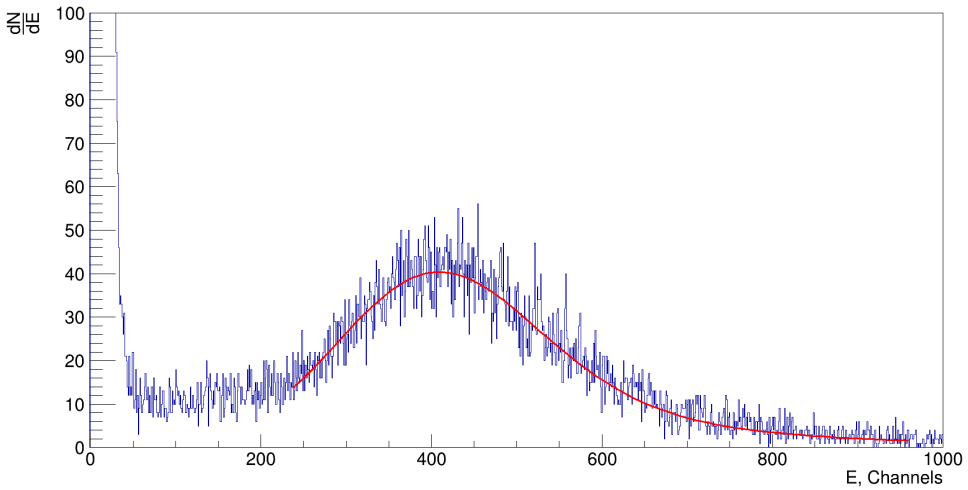

Fig. 3: Energy distribution for line 1 matted tile with convolution of Gaussian and Landau used as fitting function

of Gaussian and Landau (so-called "langaus") was used to fit the data [6]. For example, the distribution obtained for line 1 matted tile with applied fit is presented in Fig. 3. The result on the mean, the width and the integral values of the fitting area at the obtained distributions are given in Table 1.

Table 1: Mean, width and integral values of matted VS Tyvek and CKTN VS OK-72 tiles comparison

Tile	Matted VS Tyvek				CKTN MED type E VS OK-72			
	Line 1 Matted	Line 1 Tyvek	Line 3 Matted	Line 3 Tyvek	Line 1 CKTN	Line 1 OK-72	Line 3 CKTN	Line 3 OK-72
Mean, Channels	372.9	346.7	406.9	348.3	372.9	254.4	406.9	412.3
Width, Channels	28.5	30.0	30.3	27.5	28.5	17.6	30. 3	36.2
Integral	13518	13275	13993	15247	13518	10752	13993	14807

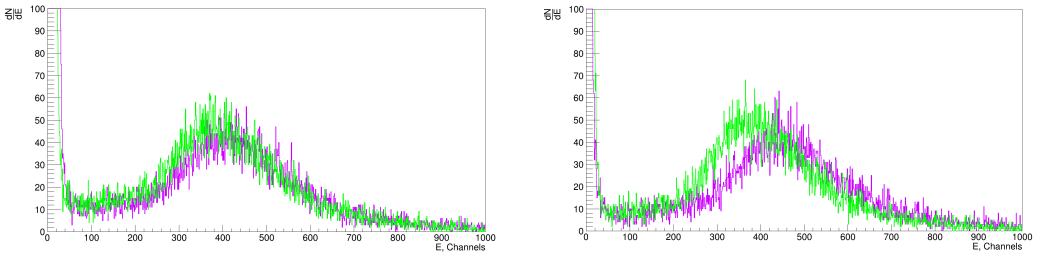

(a) (b)

Fig. 4: (*Color online*) Comparison of matted (purple) and covered with Tyvek (green) for a) line 1 b) line 3 tiles

Due to the higher peak position (from 7% and up to 15% difference) as well as the comparative simplicity in the context of mass production of

matted tiles compared to Tyvek, the option with matted ones is more appropriate.

Next step we compared two optical cements: CKTN MED type E and OK-72, optical characteristics and other parameters of the cements are presented in Table. 2.

Table 2: Optical cements and their parameters

Brand	Viscosity, cPs	Operating temperature range	Spectral characteristics	Refractive index
CKTN MED type E	$15 \cdot 10^3$	—	92-97% [7] 500 nm	1.606
OK-72	—	From -60 to +60 °C	99% [8] 400-2700 nm	1.587

In the study, we used matted tiles and different compositions of A to B components for OK-72 cement. Although OK-72 data sheet suggests using 76.24% of A component and 23.66% of B component, the mixture 70% to 30% showed better result (Fig. 5a and Fig. 5b). As for CKTN samples, in both cases (and for all comparisons) we used the same 100 of A and 3.2 of B ratio, in accordance with the data sheet. For obtained distributions of signal amplitudes we used convolution of Landau and Gauss functions. The results are presented in Table. 1.

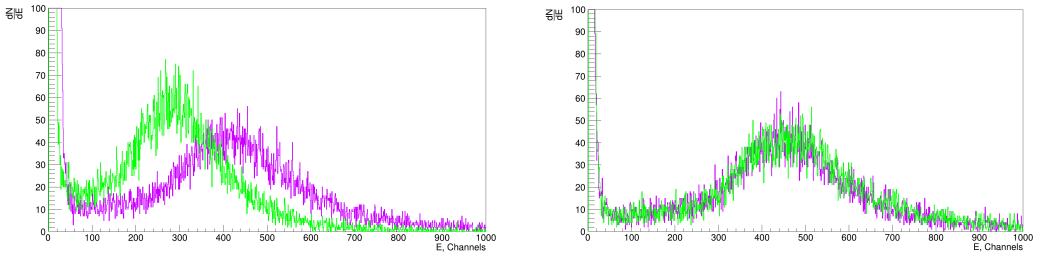

(a) (b)

Fig. 5: (*Color online*) Comparison of OK-72 (green) and CKTN (purple) for a) line 1 (76.24% of A and 23.66% of B) and b) line 3 (70% of A and 30% of B) tiles

OK-72 optical cement is easier to distribute due to its low viscosity and longer curing time (compared to CKTN type E) in terms of mass production.Considering the fact that a small difference in the ratio of two OK-72 components significantly affects the light collection, more detailed studies should be performed in the future.

In the last step, we compared Saint-Gobain Crystals BCF91AS, BCF92S, and Kuraray Y-11 WLS fibers. All samples with BCF91AS, BCF92S and Y-11 were made using CKTN MED optical cement. The study was performed with line 3 tiles. Distributions of signals amplitude are presented in Fig. 6,

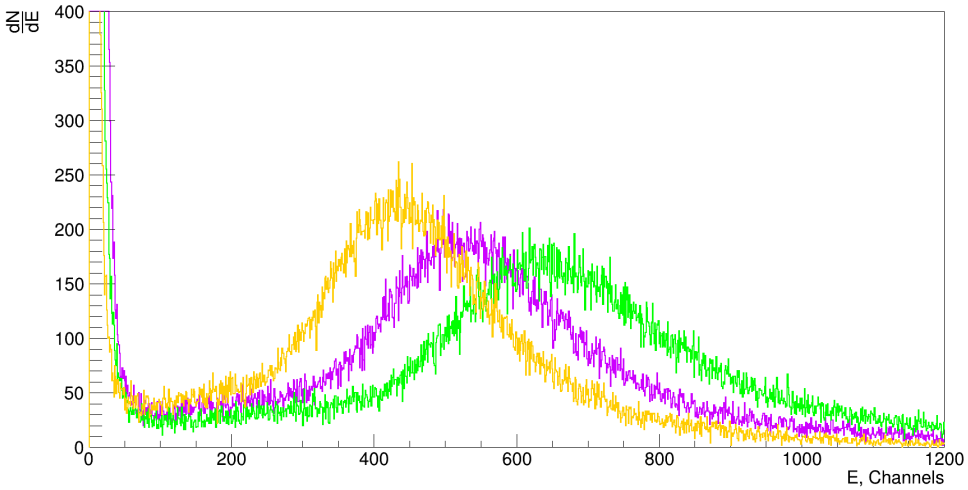

Fig. 6: (*Color online*) Comparison of BCF91AS (purple), BCF92S (yellow) and Y-11 (green)

optical parameters of fibers as well as fit results based on convolution of Landau and Gauss function are presented in Table. 3.

Table 3: Optical parameters of fibers

Fiber	Emission colour	Emission peak, nm	Decay time, ns	Att. Length, m	Mean, Channels	Width, Channels	Integral
Kuraray Y-11	green	476	7.4 [9]	>3.5	596.3	43.5	74832
SG Crystals BCF91AS	green	494	12	>3.5	481.9	35.2	72791
SG Crystals BCF92S	green	492	2.7	>3.5	402.3	24.7	67629

Due to the fact that Kuraray Y-11 fiber collects more light these fibers looks more appropriate for our detector.

Fiber parameters study

The two chosen glues were additionally studied with the central tile. In this measurement we used two tiles with BCF92S fibers of 5.5 and 36.5 cm length with CKTN cement (purple and green in Fig. 7a, respectively), and one tile with BCF92S fiber (22 cm long) and OK-72 cement (blue in Fig. 7a). With the fiber length, we assumed the length of the outer part of the fiber, the length of the WLS inside tiles of same geometry is considered to be equal within the errors.

According to the results with CKTN cement (Table 4), the fiber length affects the light collection, that is consistent with the law of light attenuation in fiber.

Another study was performed to compare different tile geometries. In the study, 3 matted tiles with CKTN cement and SG BCF92S fiber were used.

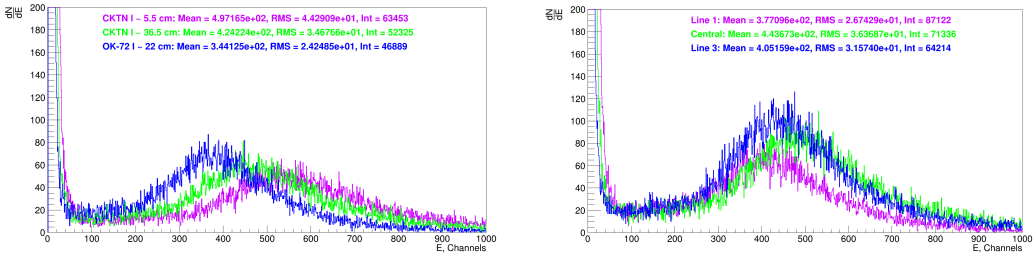

(a) (b)

Fig. 7: (*Color online*) a) Signal from central tiles with different fiber length and cement, b) Comparison of line 1, 3 and central tiles with CKTN and BCF92S

Table 4: Mean and width values of WLS lenght and different geometries comparison

Study	Central tiles fiber lenght comparison			Line 1, central and line 3 geometries comparison		
Tiles	CKTN L ≈ 5.5 cm	CKTN L ≈ 36.5 cm	OK-72 L ≈ 22.0 cm	Line 1	Central	Line 3
Mean, Channels	497.2	424.2	344.1	377.1	443.7	405.2
Width, Channels	44.3	34.7	24.2	26.7	36.4	31.6

As clearly seen in Fig. 7b the peak positions for line 1, 3 and central tiles are not the same. Using convolution of Landau and Gauss functions as fit function we derived peak position for each tile, the results are presented in Table 4.

One of the reasons for such result could be the difference between tiles in fiber curvature (Fig. 2b). Each fiber has its own bending losses. The study of bending loss requireda special tool to fix a fiber at various curvature radii (Fig. 8).

We asumed that D = 25.5 mm is a critical diameter, at which permanent damage could be inflicted to fiber. For this reason, we decided to move only through d1 to d4 diameters in the study. CAEN SP5601 led driver was used as a light source, measurements at each diameter were performed several times. Results are presented in Fig. 9.

Experimental data doesn't match well the ones from Kuraray Y-11, datasheet [10]. For deeper analysis, a more accurate additional studies are required. The study confirmed the difference in peak position between diameters d1 and d4 for one rotation of fiber inside the tool, results are presented in Table. 5.

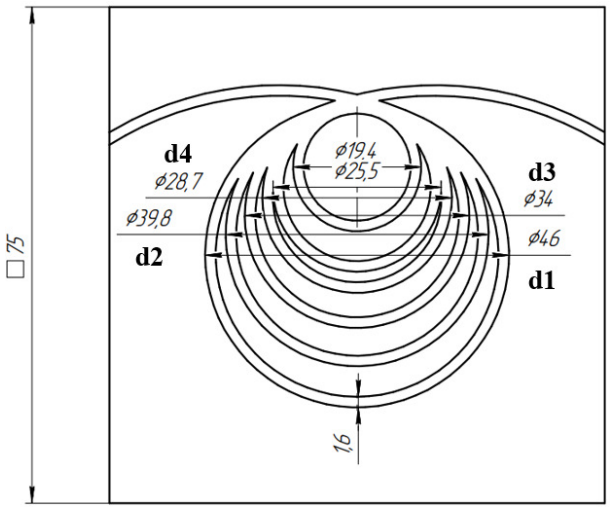

Fig. 8: Scheme of tool for bending loss study

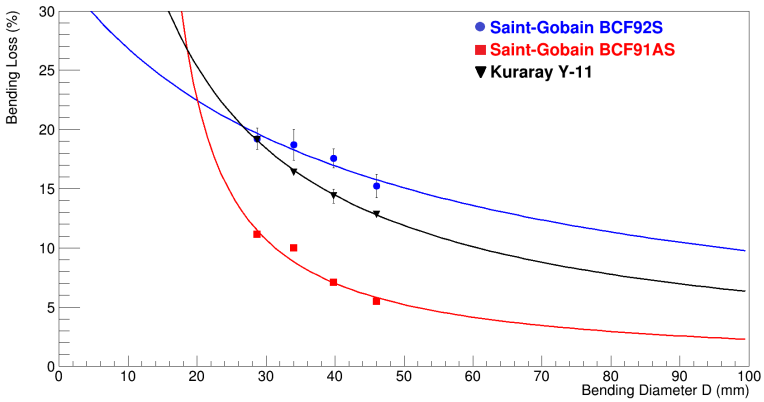

Fig. 9: Bending loss study for SGC BCF91AS, BCF92S and Kuraray Y-11 fibers

Table 5: Difference in peak positions for used fibers

Fiber	Difference in peak position between d1 and d4, %
SG BCF91AS	6.0
SG BCF92S	4.7
Kuraray Y-11	8.5

Since there are three turns of fiber inside each tile, additional studies of several rotations are required.

Conclusion

The SPD experiment at NICA will utilize scintillator-based Beam-Beam Counters in order to measure the local polarimetry and perform the monitoring of the beam collisions. In this work, the scintillator detector prototype

tests and material selection with CAEN FERS-5200 readout system has been started. The comparison of matted and Tyvek covered tiles have been done. Matted one proved to be more efficient in both ways: amount of reflected light and convenience - from 7% and up to 15% difference in peak position for light collection distributions. The comparison of CKTN MED and OK-72 optical cements have been done. The epoxy composition influence on the light collection in tiles is found for OK-72 - from 1.3% difference in favor of OK-72 to 32% difference in favor of CKTN. The comparison of SG BCF91AS, BCF92S and Kuraray Y-11 WLS fibers have been done. Y-11 proved to collect 33% more light than BCF92S and 19% more than BCF91AS The study of fibers bending loss was performed. Bending loss study doesn't fit the experimental data from Kuraray datasheet in case of Y-11 fiber.

Future plans include creating thermostabilizing technologies for SiPMs or using any kind of cryocooler. In addition, we expect to complete the transition to 1×1 mm^2 SiPMs, finalize the selection of A-B compositions for OK-72, and proceed to tests with the assembled tile sector. Further studies of the effect of fiber bending on light collecting and time resolution of the tiles are also promising.

Acknowledments

The work was funded by the Ministry of Science and Higher Education of the Russian Federation within the MEPhI Program Priority 2030. The work was partially performed using resources of NRNU MEPhI high-performance computing center.

REFERENCES

1. *Adams J., Ewigleben A., et al.* The STAR event plane detector // Nuclear Instruments and Methods in Physics Research Section A: Accelerators, Spectrometers, Detectors and Associated Equipment. 2020. Jul. V. 968. P. 163970.

2. *Abazov V.M., Abramov V., et al.* Conceptual design of the Spin Physics Detector. 2022. arXiv:2102.00442.

3. *CAEN.* FERS-5200 Front-End Readout System. `https://www.caen.it/subfamilies/fers-5200/`. Accessed: 2023-10-20.

4. *Kudenko Y., Littenberg L., Mayatski V., Mineev O., Yershov N.* Extruded plastic counters with WLS fiber readout // Nuclear Instruments and Methods in Physics Research Section A: Accelerators, Spectrometers, Detectors and Associated Equipment. 2001. august. V. 469. P. 340–346. URL: `https://doi.org/10.1088/1748-0221/11/05/t05003`.

5. *Brignoli A., Conaboy A., Dormenev V., Jimeno D., Kazlou D., Lacker H., Scharf C., Schmidt J., Zaunick H.* Wavelength-shifter coated polystyrene as an easy-to-build and low-cost plastic scintillator detector // Journal of Instrumentation. 2023. apr. V. 18, no. 04. P. P04009. URL: https://doi.org/10.1088/1748-0221/18/04/p04009.

6. *Fruehwirth R., Pernegger H., Friedl M.* Convoluted Landau and Gaussian Fitting example. https://root.cern.ch/root/html404/examples/langaus.C.html. Accessed: 2023-11-11.

7. *Artikov A., Baranov V., et al.* Optimization of light yield by injecting an optical filler into the co-extruded hole of the plastic scintillation bar // Journal of Instrumentation. 2016. may. V. 11, no. 05. P. T05003–T05003. URL: https://doi.org/10.1088/1748-0221/11/05/t05003.

8. *Vasylenko T., Mitiai E.V., Chuyko G.* Optical adhesives. Types. https://files.stroyinf.ru/Data2/1/4294836/4294836874.pdf. 1988. Accessed: 2023-10-20.

9. *Alekseev I., Danilov M., Rusinov V., Samigullin E., Svirida D., Tarkovsy E.* The performance of a new Kuraray wavelength shifting fiber YS-2 // Journal of Instrumentation. 2022. Jan. V. 17, no. 01. P. P01031.

10. *Kuraray.* Plastic Scintillating Fibers. https://www.kuraray.com/uploads/5a717515df6f5/PR0150_psf01.pdf. Accessed: 2023-10-20.